Journal of Sciences, Islamic Republic of Iran 28(2): 175 - 183 (2017) http://jsciences.ut.ac.ir
University of Tehran, ISSN 1016-1104

Bias-Induced Optical Absorption of Current Carrying Two-Orbital Quantum Dot with Strong Electron-Phonon Interaction (Polaron Regime)

A. Eskandari-asl*

Department of physics, Faculty of Sciences, University of Shahid Beheshti, Tehran, Islamic Republic of Iran

Received: 3 September 2016 / Revised: 26 October 2016 / Accepted: 25 January 2017

Abstract

The one photon absorption (OPA) cross section of a current carrying two-orbital quantum dot (QD) with strong electron-phonon interaction (polaron regime) is considered. Using the self-consistent non-equilibrium Hartree-Fock (HF) approximation, we determine the dependence of OPA cross section on the applied bias voltage, the strength of effective electron-electron interaction, and level spacing of QD. Our numerical results reveal a unique property that there are two distinct regimes for OPA. We find that for values of level spacing of QD smaller than half the strength of effective electron-electron interaction and all values of applied bias voltage, the absorption is due to the excitation of the plasmon modes of the system with low cross section, but for the values of level spacing larger than the aforementioned value, within a finite range of the applied bias voltage, set by the values of level spacing and the strength of electron-electron interaction, the OPA is due to electron transition between the two orbitals of QD with an order of magnitude larger cross section than the former case. This property results in an almost square shape cross section as a function of applied bias, for peak values of absorption at resonance frequencies.

Keywords: Two-orbital Quantum dot; Polaron regime; Bias-induced absorption; OPA cross section.

Introduction

In recent years, we have been witnessing great advances in nanotechnology, especially nano-electronics [1]. One of the challenging issues about nano devices is concerned with their interaction with external electromagnetic fields when they are driven out of equilibrium with external bias. In recent years, extensive works have been done to understand the interaction of light with nano structures for developing nano scale electro-optical devices [2-5].

A multi-orbital QD, connected to two leads and subjected to a voltage bias, is the simplest nano circuit which can be used as an electro-optical element. In such a nano-structure, the effect of electron-phonon interaction can not be ignored, especially when the coupling is strong. It is well known that strong electron-phonon coupling results in the formation of polarons in the QD which attract each other [6]. Another effect of electron-phonon interaction in the QD which must be considered is bi-stability. Several theoretical results seem to confirm the existence of bi-stability in such

* Corresponding authot: Tel: +982122431666; Fax: +982122431663; Email: amir.eskandari.asl@gmail.com

systems [6-11] and there are experimental results confirming them [12]. So, it is important to understand the effects of external bias and electron-phonon interaction, especially in the strong coupling regime (polaron regime), on the optical properties of such nano structures.

In this work, using non-equilibrium self-consistent HF approximation, we determine the dependence of OPA cross section on the level spacing, strength of effective electron-electron interaction and applied bias voltage of a two-orbital QD connected to two leads and subjected to external bias with strong electron-phonon interaction (polaron regime). We find that in terms of the aforementioned parameters there are two distinct regimes of OPA, where their cross sections differ by an order of magnitude. Based on our HF numerical results, we determine these two non-equilibrium regimes of OPA.

The paper is organized as follow: In the second section, the model Hamiltonian and the non-equilibrium self-consistent HF approximation is described and the necessary formulas for polarization, OPA cross section and the current are presented. In the third section, we report our numerical results and in the fifth section, discuss them. The non-equilibrium Green functions(GF) for the non-interacting two-orbital QD system are presented in the appendix.

Materials and Methods

Our system consists of a QD with two orbitals with different parities, connected to two leads. Each orbital is spin degenerate and strongly coupled to phonon modes of the QD. The strong electron-phonon interaction produces an attractive electron-electron interaction by forming polarons in the QD. Using the Lang-Firsov transformation[13] in the static limit, the Hamiltonian of the model in the presence of the external electromagnetic field is

$$\hat{H}_T = \hat{H}_{dot} + \hat{H}_{leads} + \hat{H}_{tun} + \hat{H}_{e-p}. \qquad (1)$$

The first two terms are, respectively, the effective Hamiltonian of a two-orbital QD and non-interacting isolated leads, given by

$$\hat{H}_{dot} = \sum_{i,\sigma} \varepsilon_i \hat{c}^{\dagger}_{i\sigma}\hat{c}_{i\sigma} - \frac{1}{2}U_0 \sum_{ij,\sigma\sigma'} \hat{n}_{i\sigma}\hat{n}_{j\sigma'}\left(1-\delta_{ij}\delta_{\sigma\sigma'}\right), \qquad (2)$$

and

$$\hat{H}_{leads} = \sum_{k\in\{R,L\},\sigma} \varepsilon_k \hat{a}^{\dagger}_{k\sigma}\hat{a}_{k\sigma}, \qquad (3)$$

where σ is the spin index, $\hat{c}_{i\sigma}$ ($\hat{c}^{\dagger}_{i\sigma}$) and $\hat{a}_{k\sigma}$ ($\hat{a}^{\dagger}_{k\sigma}$) are, respectively, the annihilation (creation) operators of electron with spin σ of the i-th orbital of QD and k-th level of leads and ε_i is the energy of i-th orbital. Moreover, $\hat{n}_{i\sigma}$ is the number operator ($\hat{c}^{\dagger}_{i\sigma}\hat{c}_{i\sigma}$) and U_0 is the strength of effective electron-electron interaction caused by the electron-phonon interaction.

The third term in Eq.1 describes the hybridization between the orbitals of QD and the two leads. For spin independent hybridization it has the form

$$\hat{H}_{tun} = \sum_{k\in\{R,L\},i,\sigma} \left(-t_{ik}\hat{a}^{\dagger}_{k\sigma}\hat{c}_{i\sigma} + h.c.\right), \qquad (4)$$

where t_{ik} s are hopping integrals where we consider them in the wide-band limit.

Finally, the last term in the Hamiltonian represents the interaction of external classical electromagnetic fields with the QD in the electric-dipole approximation. In terms of creation and annihilation operators of the QD, it is given by

$$\hat{H}_{e-p} = \sum_{\sigma} -\vec{\mu}.\vec{E}(t)\left(\hat{c}^{\dagger}_{1\sigma}\hat{c}_{2\sigma} + h.c.\right), \qquad (5)$$

where $\vec{\mu}$ is the electric-dipole matrix element between the two orbitals of QD and $\vec{E}(t)$ is the external electric field.

The bias voltage, V, is applied symmetrically to the right and left leads, thus their Fermi energies are, respectively, $\mu_L = eV/2$ and $\mu_R = -eV/2$. Moreover, the system is considered at zero temperature and we choose the system of units that $e = \hbar = 1$.

The HF Approximation

To determine the optical properties of our model, we use the Keldysh formalism of non-equilibrium (contour-ordered) Green's functions (NEGF) which is an extremely useful method for studying the non-equilibrium properties of many-body systems. Within the various approximations, we limit ourselves to the HF self-consistent method. This method is sufficiently simple and computationally less demanding and at the same time produces semi quantitative results.

Green's functions provide us with expectation values of all one-body observables such as polarization, density and the current. They satisfy the Dyson equations [14]

$$G_c = G_c^0 + G_c^0 \Sigma_c G_c, \qquad (6)$$

where G_c and G_c^0 are, respectively, the contour-ordered exact and non-interacting GFs which for the QD are defined as

$$G_{c,ij}(\tau,\tau') = -i\left\langle T_c\left(\hat{c}_{H,i\sigma}(\tau)\hat{c}^{\dagger}_{H,i\sigma}(\tau')\right)\right\rangle, \quad i,j=1,2 \tag{7}$$

and

$$G^{0}_{c,ij}(\tau,\tau') = -i\left\langle T_c\left(\hat{c}_{H,i\sigma}(\tau)\hat{c}^{\dagger}_{H,i\sigma}(\tau')\right)\right\rangle_0, \quad i,j=1,2 \tag{8}$$

where Σ_c is the proper self-energy and $\hat{c}_{H,i\sigma}(\tau)$s ($\hat{c}^{\dagger}_{H,i\sigma}(\tau)$s) are the annihilation (creation) operators in the Heisenberg representation on the Keldysh time contour.

Using the analytical continuation of Langreth[14], we can express the Dyson equations in terms of standard retarded (G^r, G^{0r}, Σ^r), advanced (G^a, G^{0a}, Σ^a), lesser ($G^<, G^{0<}, \Sigma^<$) and greater ($G^>, G^{0>}, \Sigma^>$) GFs and proper self-energies. Since for the Hamiltonian, $\hat{H}_T$, the GFs and self-energies are diagonal in spin space, we have dropped the spin indices. Within the HF approximation the resulting equations for the GFs when $\hat{H}_{e-p}$ is ignored, are

$$\hat{G}^r(\omega) = \left[\left(\hat{G}^{0r}(\omega)\right)^{-1} - \hat{\Sigma}^r_{HF}\right]^{-1}, \tag{9}$$

$$\hat{G}^a(\omega) = \hat{G}^r(\omega)^{\dagger}, \tag{10}$$

and

$$\hat{G}^<(\omega) = \hat{G}^r(\omega)\hat{\Sigma}^<_{leads}(\omega)\hat{G}^a(\omega), \tag{11}$$

where $\hat{\Sigma}^<_{leads}(\omega)$ is the lesser self-energy due to the leads which is defined in the appendix and $\hat{\Sigma}^r_{HF}$, the HF retarded self-energy, is given by

$$\hat{\Sigma}^r_{HF} = \begin{pmatrix} -U_0(n_{1\sigma}+2n_{2\sigma}) & r_\sigma \\ r^*_\sigma & -U_0(n_{2\sigma}+2n_{1\sigma}) \end{pmatrix}, \tag{12}$$

where

$$n_{i\sigma} = -i\int\frac{d\omega}{2\pi}G^<_{ii}(\omega), \qquad \sigma=\uparrow,\downarrow, \tag{13}$$

and

$$r_\sigma = -iU_0\int\frac{d\omega}{2\pi}\left(G^r_{12}(\omega)+G^<_{12}(\omega)\right). \tag{14}$$

Using the relation

$$\int\frac{d\omega}{2\pi}G^r_{12}(\omega) = \frac{-i}{2}\left\langle\left\{\hat{c}_{1\sigma},\hat{c}^{\dagger}_{2\sigma}\right\}\right\rangle = 0, \tag{15}$$

in Eq.14, we have

$$r_\sigma = -iU_0\int\frac{d\omega}{2\pi}G^<_{12}(\omega). \tag{16}$$

Furthermore, r_σ is real, so $r_\sigma = r^*_\sigma$.

Polarization and Linear Polarizability

The polarization of QD is defined by

$$\vec{P}(t) = \vec{\mu}\sum_\sigma\left\langle\hat{c}_{H,1\sigma}(t)\hat{c}^{\dagger}_{H,2\sigma}(t)+\hat{c}_{H,2\sigma}(t)\hat{c}^{\dagger}_{H,1\sigma}(t)\right\rangle. \tag{17}$$

Using equal time anti-commutation properties of annihilation and creation operators, Eq.17 can be written as[3]

$$\vec{P}(t) = 4\,\mathrm{Im}\left(\vec{\mu}\tilde{G}^<_{12}(t,t)\right), \tag{18}$$

where $\tilde{G}^<_{12}(t,t)$ is the lesser GF between the two orbitals of QD when $\hat{H}_{e-p}$ is taken into account.

Since, we are interested in the OPA cross section, we determine $\vec{P}(t)$ to first order in $\vec{E}(t)$. The contour-ordered GF to first order in $\hat{H}_{e-p}$ is

$$\hat{\tilde{G}}(\tau,\tau') = \int d\tau_1\hat{G}(\tau,\tau_1)\hat{h}_{e-p}(\tau_1)\hat{G}(\tau_1,\tau'), \tag{19}$$

where all the τ s lie on the Keldysh time contour, $\hat{G}$ represents the HF GFs of the QD, and $\hat{h}_{e-p}$ is

$$\hat{h}_{e-p}(\tau) = \begin{pmatrix} 0 & -\vec{\mu}.\vec{E}(\tau) \\ -\vec{\mu}.\vec{E}(\tau) & 0 \end{pmatrix}. \tag{20}$$

Using the Langreth rules and doing the Fourier transformations, the first order polarization for $\vec{E}$ in the direction of $\vec{\mu}$ could be written as

$$P^{(1)}(\omega) = 2i\,\mu^2E(\omega)\left[\gamma(-\omega,\omega)-\gamma^*(\omega,-\omega)\right], \tag{21}$$

where $E(\omega)$ is the Fourier transform of the electric field and

(22)

$$\gamma(-\omega,\omega) = \int\frac{d\omega'}{2\pi}[G^r_{12}(\omega+\omega')G^<_{12}(\omega')+G^r_{11}(\omega+\omega')G^<_{22}(\omega') + G^<_{12}(\omega+\omega')G^a_{12}(\omega')+G^<_{11}(\omega+\omega')G^a_{22}(\omega')].$$

In terms of $\gamma(-\omega,\omega)$, the frequency dependent OPA cross section is

$$\sigma(\omega) = \frac{8\pi\omega\mu^2}{c}\mathrm{Re}\left[\gamma(-\omega,\omega)-\gamma^*(\omega,-\omega)\right]. \tag{23}$$

Furthermore, the total current in the absence of the

last term in the Hamiltonian has the form

$$I=\frac{ie}{\hbar}\int_{\mu_R}^{\mu_L}\frac{d\omega}{2\pi}Tr\left[\hat{\Gamma}\left(\hat{G}^r(\omega)-\hat{G}^a(\omega)\right)\right], \quad (24)$$

where the trace is taken over the orbital degrees of freedom of the QD, a factor of 2 is already taken into account for spin, and $\hat{\Gamma}$ is given by[14]

$$\Gamma_{ij}(\varepsilon)=2\pi\sum_k t_{ik}t_{jk}^*\delta(\varepsilon-\varepsilon_k), \quad (25)$$

which in the wide-band approximation is independent of ε. Furthermore, we take all Γ_{ij} equal to Γ.

Results

In this section we present and discuss our results. Within the HF approximation, it is well known that the Hamiltonian, $\hat{H}_T$, shows bi-stability [7]. Our numerical results in the sequel belong to the lower branch of bi-stability curve for two distinct cases, the degenerate ($\varepsilon_1=\varepsilon_2$) and non-degenerate ($\varepsilon_1\neq\varepsilon_2$) QDs.

Degenerate QD

For simplicity, we take $\varepsilon_1=\varepsilon_2=0$. It would be more convenient to use another single particle orbitals for QD. Doing the following transformation on the annihilation and creation operators of the QD,

$$\hat{d}_{1\sigma}=\frac{1}{\sqrt{2}}(\hat{c}_{1\sigma}+\hat{c}_{2\sigma}),\quad \hat{d}^\dagger_{1\sigma}=\frac{1}{\sqrt{2}}(\hat{c}^\dagger_{1\sigma}+\hat{c}^\dagger_{2\sigma}), \quad (26)$$

and

$$\hat{d}_{2\sigma}=\frac{1}{\sqrt{2}}(\hat{c}_{1\sigma}-\hat{c}_{2\sigma}),\quad \hat{d}^\dagger_{2\sigma}=\frac{1}{\sqrt{2}}(\hat{c}^\dagger_{1\sigma}-\hat{c}^\dagger_{2\sigma}), \quad (27)$$

The Hamiltonian of the QD, $\hat{H}_{dot}$, retains its form, but the left and right leads decouple from the transformed second orbital of the QD. This decoupling makes the Fock term, Eq.16, identically zero. The first, third and the last terms of the total Hamiltonian in the new basis are, respectively,

$$\hat{\tilde{H}}_{dot}=-\frac{1}{2}U_0\sum_{ij,\sigma\sigma'}\hat{\tilde{n}}_{i\sigma}\hat{\tilde{n}}_{j\sigma'}\left(1-\delta_{ij}\delta_{\sigma\sigma'}\right), \quad (28)$$

$$\hat{\tilde{H}}_{tun}=\sum_{k\in\{R,L\},\sigma}\left(-\sqrt{2}t_k\hat{a}^\dagger_{k\sigma}\hat{d}_{1\sigma}+h.c.\right), \quad (29)$$

and

$$\hat{\tilde{H}}_{e-p}=\sum_\sigma -\vec{\mu}.\vec{E}(t)\left(\hat{\tilde{n}}_{1\sigma}-\hat{\tilde{n}}_{2\sigma}\right), \quad (30)$$

where it is assumed that $t_{1k}=t_{2k}=t_k$ and $\hat{\tilde{n}}_{i\sigma}=\hat{d}^\dagger_{i\sigma}\hat{d}_{i\sigma}$ for i=1,2 and $\sigma=\uparrow,\downarrow$.

In the new basis, the GFs in the Hartree approximation can be determined analytically. It is a straight forward calculation to show that the non-zero GFs are

$$g^r_{11}(\omega)=g^{a*}_{11}(\omega)=\frac{1}{\omega+(\tilde{n}_{1\sigma}+2\tilde{n}_{2\sigma})U_0+i\Gamma}, \quad (31)$$

$$g^r_{22}(\omega)=g^{a*}_{22}(\omega)=\frac{1}{\omega+(2\tilde{n}_{1\sigma}+\tilde{n}_{2\sigma})U_0+i0^+}, \quad (32)$$

$$g^<_{11}(\omega)=\frac{i\Gamma\sum_{\alpha\in\{R,L\}}\theta(\mu_\alpha-\omega)}{\left[\omega+(\tilde{n}_{1\sigma}+2\tilde{n}_{2\sigma})U_0\right]^2+\Gamma^2}, \quad (33)$$

$$g^<_{22}(\omega)=i\pi\delta\left[\omega+(2\tilde{n}_{1\sigma}+\tilde{n}_{2\sigma})U_0\right]\sum_{\alpha\in\{R,L\}}\theta(\mu_\alpha-\omega), \quad (34)$$

and the greater GFs are given by

$$g^>_{ii}(\omega)=g^r_{ii}(\omega)-g^a_{ii}(\omega)+g^<_{ii}(\omega),\quad i=1,2 \quad (35)$$

where $\theta(\mu_\alpha-\omega)$ is the Heaviside step function and $\hat{\tilde{n}}_{i\sigma}$s are the solutions of the following coupled integral equations:

$$\tilde{n}_{i\sigma}=-i\int\frac{d\omega}{2\pi}g^<_{ii}(\omega),\quad i=1,2,\quad \sigma=\uparrow,\downarrow, \quad (36)$$

For $n_{2\sigma}$, the integral can be done and we have

$$\tilde{n}_{2\sigma}=\frac{1}{2}\left[1+\theta\left(-\frac{V}{2}+(2\tilde{n}_{1\sigma}+\tilde{n}_{2\sigma})U_0\right)\right],\quad \sigma=\uparrow,\downarrow. \quad (37)$$

Furthermore, the polarization, Eq.17, becomes

$$\vec{P}(t)=2i\vec{\mu}\left[g^<_{11}(t,t)-g^<_{22}(t,t)\right]. \quad (38)$$

Using the self-consistent solutions of Eqs.36 and 37 with Eq.24 for the current, we have depicted the populations of the two orbitals , $\tilde{n}_1$ and $\tilde{n}_2$, of the QD and the current, I, as functions of external bias, V , for three values of $U_0/\Gamma=2.0,4.0$ and 6.0 in Figs. 1a and 1b. The OPA cross section for $U_0/\Gamma=4.0$ and $eV/\Gamma=20.0$ as a function of $\hbar\omega/\Gamma$ is depicted in Fig. 2. The peaks are due to the excitation of plasmon

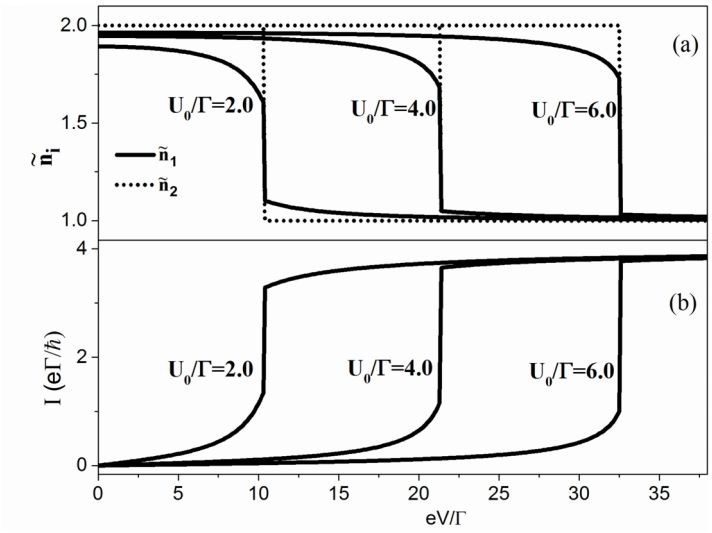

Figure 1. (a)The electron populations and (b)the currents, for the degenerate case, for $U_0/\Gamma = 2.0, 4.0$ and 6.0, as functions of the bias voltage.

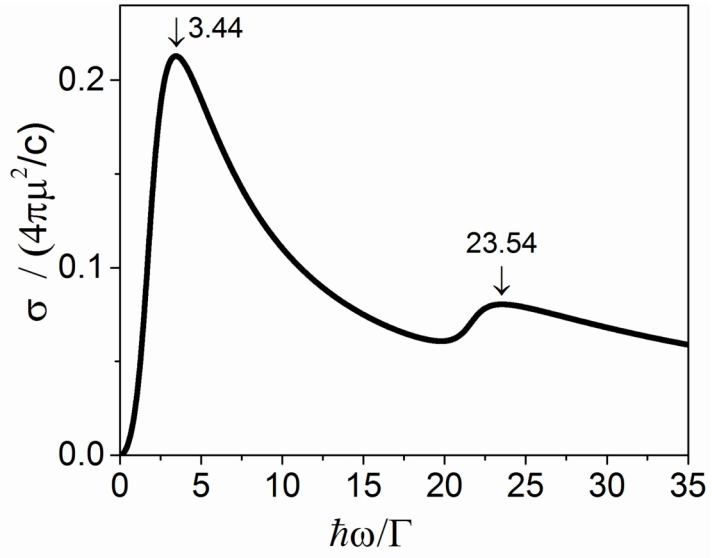

Figure 2. The OPA cross section of the degenerate case, as a function of frequency for $U_0/\Gamma = 4.0$ and $eV/\Gamma = 20.0$. The arrows indicate the resonance frequencies and c is the speed of light.

modes of the system. Since the polarization in the transformed basis, Eq.38, is proportional to the difference between the electron populations of the two transformed orbitals and $\hat{H}_{e-p}$ (Eq.30), couples the incoming electric field to the electron populations of the orbitals, to linear order in the electric field the change in the polarization is proportional to the density-density response function of the QD, whose collective excitations are the plasmon modes of the system. So the absorption peaks in Fig. 2 are due to excitations of plasmons.

Non-Degenerate QD

In this case, we set $\varepsilon_1 = -\varepsilon_2 = \delta$ and for any values of U_0 and V , we solve Eqs. 9-13 and 16 self-consistently. In Figs. 3a, 3b and 3c, the populations of the two orbitals of QD and the current as functions of external bias voltage are depicted for $U_0/\Gamma = 4.0$ and $\delta/\Gamma = 1.5$ and 3.0. For $\delta/\Gamma = 1.5$, the I-V curve has a step shape, but for $\delta/\Gamma = 3.0$ it consists of two steps. This behavior of I-V curve is due to the electron populations of the two orbitals of QD. For values of

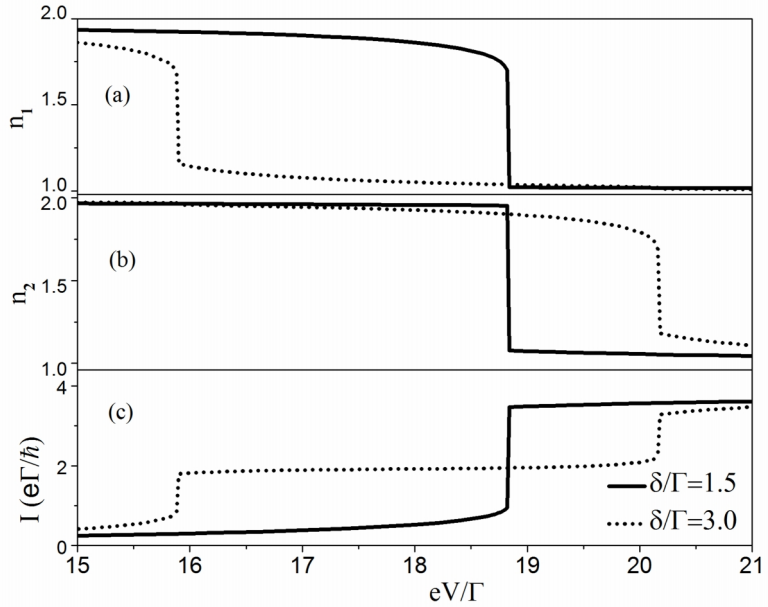

Figure 3. (a), (b) and (c) are, respectively, the electron populations of the two orbitals of QD and the current as functions of the bias voltage for $U_0/\Gamma = 4.0$ and $\delta/\Gamma = 1.5$ and 3.0.

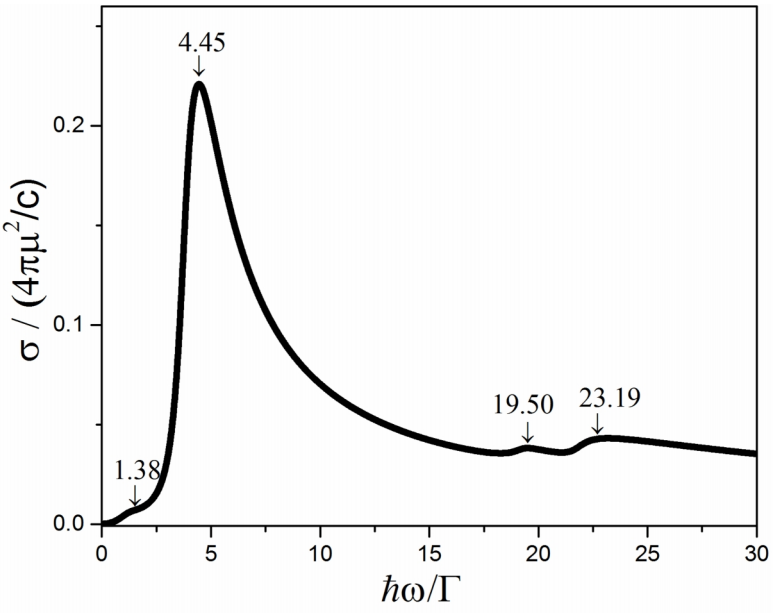

Figure 4. The OPA absorption cross section for $U_0/\Gamma = 4.0, \delta/\Gamma = 1.5$ and $eV/\Gamma = 18.0$ as a function of the frequency. The arrows indicate the resonance frequencies and c is the speed of light.

$\delta < U_0/2$, when the bias voltage is increased, the two orbitals get populated almost with the same number of electrons, Figs. 3a and 3b. For $eV/\Gamma < 18.82$ the two orbitals are almost filled and small current can pass through the dot. For $eV/\Gamma > 18.82$ the two orbitals are almost half filled and the dot can pass larger current. As the δ increases above $U_0/2$, the electron populations of the two orbitals as functions of applied bias voltage become different. This behavior could be explained by noticing that for an orbital to be filled, its effective energy ,that is, its energy plus the Hartree energy (see Eq.12), should lie below the Fermi energy of the right lead. The effective energies of the higher and lower orbitals of the QD are, respectively, $\delta - U_0(n_{1\sigma} + 2n_{2\sigma})$ and $-\delta - U_0(n_{2\sigma} + 2n_{1\sigma})$. If we

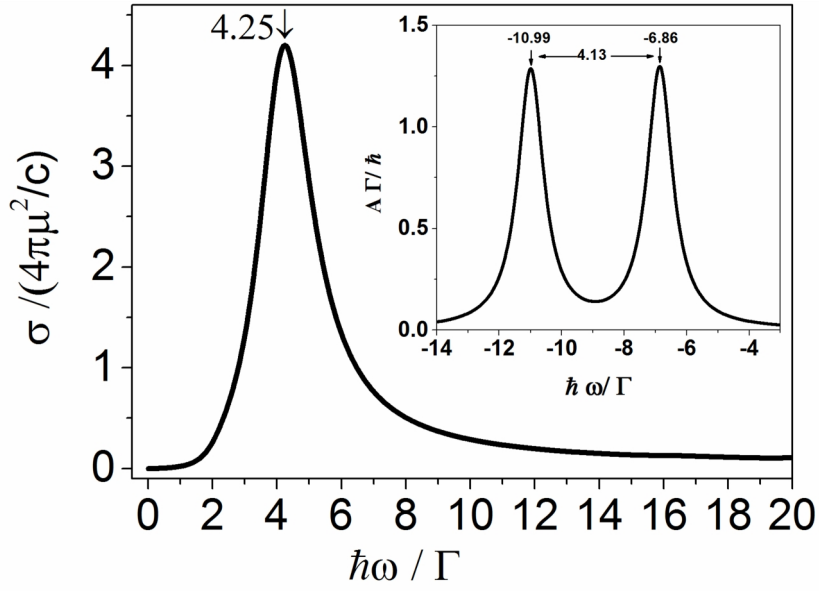

Figure 5. The absorption cross section for $U_0/\Gamma = 4.0$, $\delta/\Gamma = 3.0$ and $eV/\Gamma = 18.0$ as a function of the frequency. The inset is the one particle spectral function for the two levels of QD. c is the speed of light.

roughly assume that the filled orbitals are completely filled, the higher orbital would remain filled up to the bias voltage for which the Fermi energy of the right lead is approximately equal to its effective energy, $\delta - 3U_0$. Therefor, at applied bias approximately equal to $2(3U_0 - \delta)$, the first step emerges. Increasing the applied bias, the higher orbital becomes almost half filled and up to applied bias of $2(2U_0 + \delta)$, where $2(2U_0 + \delta) > 2(3U_0 - \delta)$, the lower orbital remains approximately filled. At the above applied bias the Fermi energy of the right lead becomes equal to the effective energy of the lower orbital where the second step emerges. Increasing the applied bias further, the two orbitals of QD become almost half filled.

The relation $2(2U_0 + \delta) > 2(3U_0 - \delta)$ can be satisfied only for $\delta > U_0/2$. Therefore, $\delta \approx U_0/2$ is a threshold for the I-V curve to have two steps. From the above consideration, we conclude that for level spacing above the threshold, the range of applied bias, eV, where the lower orbital is almost filled and the other orbital approximately half filled is $2(3U_0 - \delta) < eV < 2(2U_0 + \delta)$.

In Fig. 4, we show the OPA cross section for the case where $\delta < U_0/2$ ($U_0/\Gamma = 4.0, \delta/\Gamma = 1.5$ and $eV/\Gamma = 18.0$). Since the populations of the two orbitals are almost equal, see Figs. 3a and 3b, the absorption peaks are due to the plasmon excitations.

In Fig. 5, the OPA cross section for $U_0/\Gamma = 4.0$, $\delta/\Gamma = 3.0$ (above threshold $\delta \approx U_0/2$) and $eV/\Gamma = 18.0$ is depicted and the inset shows one-particle spectral density of QD, $A(\omega) = -\frac{2}{\pi}\sum_{ii} \mathrm{Im}\left[G^r_{ii}(\omega)\right]$. The OPA cross section has a main peak at $\hbar\omega/\Gamma = 4.25$ with a height which is one order of magnitude larger than the previous case where $\delta < U_0/2$, and its energy is approximately equal to the energy difference of the two peaks in the one-particle spectral density (see the inset of Fig. 5). This peak is due to the absorption of a photon by the electrons in the low energy orbital of the QD, making transition to the other orbital. The reason that such a transition occurs in this case and not in the former case (Fig. 4) is that the level populations of the two orbitals of the QD differ substantially, see Figs.3a and 3b. In Fig.6, for $U_0/\Gamma = 4.0$ and $\delta/\Gamma = 2.5$and 3.0, we have plotted the heights of main peaks of OPA cross sections as functions of external bias voltage. In this regime, the resulting curve has an almost square shape with an approximate width of $4\delta - 2U_0$. Considering the orbitals populations and the currents as functions of bias, we observe large absorption for the range of applied bias voltage that lies between the two steps of the I-V curve. Also, within this range of applied bias the electron populations of the two orbitals of QD show

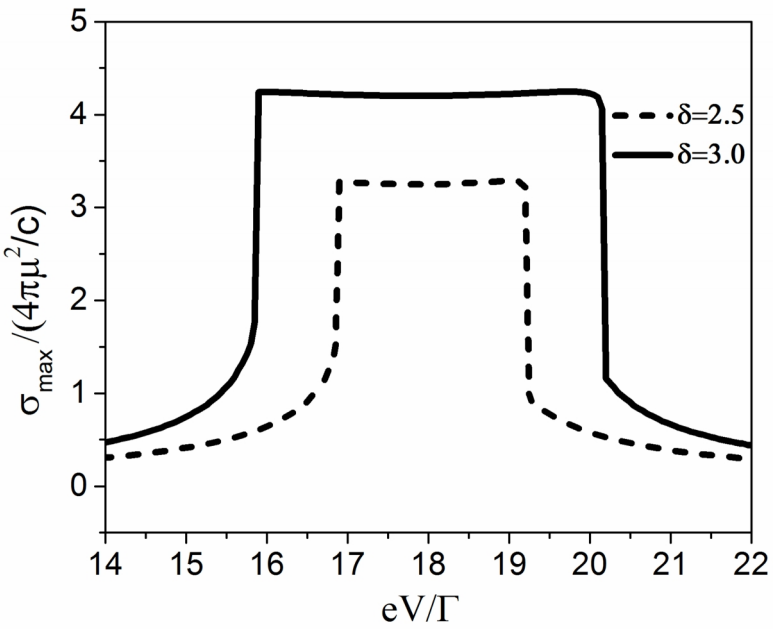

Figure 6. The heights of the main peaks in OPA cross sections for $U_0/\Gamma = 4.0$ and $\delta/\Gamma = 2.5$ and 3.0, as functions of the bias voltage. c is the speed of light and the widths of curves are approximately equal to $4\delta - 2U_0$.

maximum difference. We have also calculated the OPA cross section on the upper branch of bi-stability curve, the results do not differ significantly from the reported lower branch.

Discussion

We have investigated the OPA properties of a current carrying two-orbital QD in the limit of strong electron-phonon interaction (polaron regime). Our numerical results which are based on the non-equilibrium self-consistent HF approximation, show that this simple nano-structure has two distinct regimes of OPA, where their cross sections differ by an order of magnitude. Furthermore, based on our numerical results for OPA cross sections and their dependence on the applied bias voltage, strength of effective electron-electron interaction and the level spacing of QD, we have determined in terms of the aforementioned parameters the two regimes of OPA, where one is associated to the plasmon excitations of system and the other one to the inter-dot transition of electrons.

We conclude our work by noting that such an intriguing optical property which is the manifestation of non-equilibrium state of system, could be of great practical interest for electro-optical elements at nano-scale.

Appendix. The Non-Equilibrium Green Functions of the Non-Interacting Two-Orbital QD

In this appendix, we present the expressions for different non-equilibrium GFs of two-orbital QD in the non-interacting case.

The retarded and lesser self-energies of the leads in the wide band approximation are, respectively [14],

$$\Sigma^{r}_{leads,ij} = -\frac{i}{2}\Gamma_{ij}, \qquad i,j = 1,2, \tag{A.1}$$

and

$$\Sigma^{<}_{leads,ij}(\omega) = \frac{i}{2}\Gamma_{ij}\sum_{\alpha\in\{R,L\}}\theta(\mu_\alpha - \omega), \qquad i,j = 1,2. \tag{A.2}$$

The retarded, advanced and lesser GFs can be determined using the following equations:

$$\hat{G}^{0r}(\omega) = \left[(\omega + i\,0^{+})I - \hat{h}_{dot} - \hat{\Sigma}^{r}_{leads}\right]^{-1}, \tag{A.3}$$

$$\hat{G}^{0a}(\omega) = \hat{G}^{0r}(\omega)^{\dagger}, \tag{A.4}$$

and

$$\hat{G}^{0<}(\omega) = \hat{G}^{0r}(\omega)\hat{\Sigma}^{<}_{leads}(\omega)\hat{G}^{0a}(\omega), \tag{A.5}$$

where all the GFs and self energies are two by two matrices and $\hat{h}_{dot}$ is

$$\hat{h}_{dot} = \begin{pmatrix} \varepsilon_1 & 0 \\ 0 & \varepsilon_2 \end{pmatrix}. \quad \text{(A.6)}$$

References

1. Cuevas J., Scheer E., Molecular Electronics: An Introduction to Theory and Experiment, *World Sci., Singapore* (2010).
2. Tame M. S., McEnery K. R., Özdemir Ş. K., Lee J., Maier S. A., and Kim M. S., Quantum plasmonics. *Nat. Phys.*, **9**(6): 329-340 (2013).
3. White A. J., Sukharev M., and Galperin M., Molecular nanoplasmonics: Self-consistent electrodynamics in current-carrying junctions. *Phys. Rev. B.*, **86**(20): 205324 (2012).
4. Galperin M., and Nitzan A., Molecular optoelectronics: the interaction of molecular conduction junctions with light. *Phys. Chem. Chem. Phys.*, **14(**26): 9421-9438 (2012).
5. Park T. H., and Galperin, M., Charge-transfer contribution to surface-enhanced Raman scattering in a molecular junction: Time-dependent correlations. *Phys. Rev. B.*, **84**(7): 075447 (2011).
6. Alexandrov A. S., Bratkovsky A. M., and Williams R. S., Bistable tunneling current through a molecular quantum dot. *Phys. Rev. B.*, **67**(7): 075301 (2003).
7. Galperin M., Nitzan A., and Ratner M. A., The non-linear response of molecular junctions: the polaron model revisited. *J. Phys. Cond. Mat.*, **20**(37): 374107 (2008).
8. Alexandrov A. S., and Bratkovsky A. M., Polaronic memory resistors strongly coupled to electrodes. *Phys. Rev. B.*, **80**(11): 115321 (2009).
9. Albrecht K. F., Wang H., Mühlbacher L., Thoss M., and Komnik A., Bistability signatures in nonequilibrium charge transport through molecular quantum dots. *Phys. Rev. B.*, **86**(8): 081412 (2012).
10. Wilner E.Y., Wang H., Thoss M. and Rabani E., Phonon dynamics in correlated quantum systems driven away from equilibrium. *Phys. Rev. B.*, **90**(11): 115145 (2014).
11. Klatt J., Mühlbacher L., and Komnik A., Kondo effect and the fate of bistability in molecular quantum dots with strong electron-phonon coupling.*Phys. Rev. B.*, **91**(15): 155306 (2015).
12. Liljeroth P., Repp J., and Meyer G., Current-induced hydrogen tautomerization and conductance switching of naphthalocyanine molecules. *Science*, **317**(5842):1203-1206 (2007).
13. Lang I. G., and Firsov Y. A., Kinetic theory of semiconductors with low mobility. *J. Exp. Theor. Phys.*, **16**: 1301 (1963).
14. Stefanucci G., and Van Leeuwen R., Nonequilibrium Many-Body Theory of Quantum Systems: A Modern Introduction. *Camb. Univ. Press* (2013).